New Journal of Physics
An Institute of Physics and Deutsche Physikalische Gesellschaft Journal

The role of neutrinos, rotations and magnetic fields in collapse-driven supernovae

Shoichi Yamada[1], **Kei Kotake**[2] **and Tatsuya Yamasaki**[3]

[1] Science and Engineering, Waseda University, 3-4-1 Okubo, Shinjuku, Tokyo 169-8555, Japan
[2] Department of Physics, School of Science, University of Tokyo, 7-3-1, Hongo, Bunkyo, Tokyo 113-0033, Japan
[3] Department of Astronomy, Faculty of Science, Kyoto University, Sakyo, Kyoto 606-8502, Japan
E-mail: shoichi@waseda.jp

New Journal of Physics **6** (2004) 79
Received 2 May 2004
Published 9 July 2004
Online at http://www.njp.org/
doi:10.1088/1367-2630/6/1/079

Abstract. Neutrinos are considered to be one of the most important ingredients of collapse-driven supernovae. In the last couple of years, we have seen major progress in both numerical modelling and microphysical understanding of supernova neutrinos. The successful explosion, however, is still elusive. In the former half of this article, we give a brief overview on the current status of the theoretical understanding of the supernova mechanism. In the latter half, we present some new results on multi-dimensional aspects such as rapid rotations, strong magnetic fields and resultant anisotropic neutrino heating, to which our group is currently paying particular attention as an important element for successful explosions. We employ both statical and dynamical approaches. The gravitational waves obtained in the dynamical computations are summarized in an appendix.

PII: S1367-2630(04)80233-7

Contents

1. Overview

Substantial effort has been devoted to the study of the mechanism of collapse-driven supernovae during the last 40 years [1]. We know for sure from the observations of SN1987A that they are associated with the death of massive stars ($\gtrsim 10 M_\odot$) [2] and that they emit a large number of neutrinos which corresponds to the typical gravitational binding energy of the neutron star over the diffusion time scale of neutrinos in the hot and dense supernova core [3]. Unfortunately, however, we are still not able to tell exactly what drives this explosive phenomenon. Even the most elaborate theoretical models have so far failed to produce successful explosions [4]–[9].

Collapse-driven supernovae are important astrophysical objects in various respects. Most of the heavy elements are synthesized in stars and distributed to the interstellar space by the supernova explosion and the chemical evolution of the galaxy occurs as a result [10]. The collapse-driven supernovae are thought to be one of the most promising sites for r-process [11]. Not only neutrinos but also gravitational waves will be emitted and might be observed if the supernova is not spherically symmetric due to rapid rotation, for example, making the supernova the important target of the looming neutrino and gravitational astronomy [12, 13]. Since the dynamics of the supernova is mainly dictated by microphysics such as weak interactions and nuclear physics as explained below, the revelation of the supernova mechanism will be led or followed by a better understanding of these microphysics.

Recently, the fate of massive stars has attracted considerable attention. This is mainly due to the general recognition that, at least, some of the long-duration gamma-ray bursts (GRB) are associated with the collapse of massive stars and supernova-like events [14]. In particular, the observation of GRB030329/SN2003dh is convincing [15]. The fact that the accompanying supernovae are in general more energetic (they are frequently referred to as 'hypernovae' in the literature and we also employ this term in this sense here) than the canonical collapse-driven supernova is another reason for this frenzy [16]. The comparison of the event rates seems to suggest that most of GRB are accompanied by a hypernova [17]. Although it is supposed that the GRB/hypernova system is partly a result of the black-hole formation, it is not clear how this is

the case. In this context, it is very interesting to know where the boundary between the formation of a neutron star and that of a black hole [18] exists and what causes the difference between the ordinary supernova and the hypernova [19]. All those questions remain to be answered.

In this paper, we focus on the ordinary supernova which will lead to neutron star formation. This may be corresponding to the progenitor mass of about 10–20$M_\odot$ [19, 20]. As will be explained below, the most promising current scenario is the neutrino-driven explosion. In this section, we will first review this scenario briefly, summarizing recent progress in theoretical studies. Then we will discuss some possible boosters, which are expected to help neutrinos to trigger explosions. We pay particular attention to the rotation-induced asymmetry of neutrino emission. We also mention stellar magnetic fields at the end of this section. Our new results on these subjects will be presented in the next two sections.

1.1. The importance of neutrino

The collapse-driven supernova is initiated by the collapse of the stellar core. The pressure deficit due to electron captures and photo-dissociations of nuclei triggers the radial instability. The gravitational stability is not recovered until the nuclear density is reached and the equation of state (EOS) becomes very stiff. In the meantime, the neutrinos emitted by the electron capture are trapped in the core and cannot get out on the dynamical time scale after the density becomes $\gtrsim 10^{11}\,\mathrm{g\,cm^{-3}}$ and the mean free path due to the coherent scattering on nuclei becomes much smaller than the core size. When the core bounce occurs at the central density of a few times the nuclear saturation density, the liberated gravitational energy of $\sim 10^{53}$ erg is stored mostly as the internal energy of the core and is radiated away much later as the trapped neutrinos are getting out of the core on the diffusion time scale [3].

The collapsing core consists of the so-called inner and outer cores; the former contracts in a subsonic and homologous way while the latter falls supersonically on to the former. The bounce of the inner core generates a shock wave at the boundary of these two cores. As the shock wave propagates outwards through the outer core, neutrino emissions and photo-dissociations of nuclei deprive the shock wave of the energy. In the recent sophisticated simulations [4]–[9], the shock wave stalls and becomes an accretion shock inside the core. How far the shock wave can go before stagnation depends on the proportion of the inner and outer cores, which is in turn determined by the electron captures in the collapsing phase [21]. The rates of electron captures on nuclei had been one of the uncertainties in nuclear physics until quite recently [22]. The more suppressed the electron captures are and, as a result, the more lepton-rich the inner core is, the farther the shock wave can go and the easier the explosion may be. The large-scale shell-model calculations by Langanke *et al* [21] have shown that the electron captures proceed further than expected for the standard approximate treatment. Now there seems to be no chance for prompt explosions (see section 1.3, however).

To produce explosions, the stalled shock must be somehow revived. As mentioned above, the neutrino heating is supposed to be the most promising mechanism for that. Due to the neutrino trapping, most of the energy liberated by the gravitational collapse is stored as internal energy in the core and is carried away together with the lepton number by neutrinos diffusing out of the core on the time scale much longer than the dynamical time scale. Although all flavours of neutrinos are emitted, the electron-type neutrinos and anti-neutrinos are mainly responsible for the heating of the matter behind the shock wave via absorptions on nucleons, $\nu_\mathrm{e} + \mathrm{n} \rightarrow \mathrm{p} + \mathrm{e}$ and $\bar{\nu}_\mathrm{e} + \mathrm{p} \rightarrow \mathrm{n} + \mathrm{e}^+$. The merit of the neutrino-heating mechanism is that neutrinos transport a

great amount of energy equal to the gravitational binding energy of a neutron star, $\sim 10^{53}$ erg, which is about a 100 times the typical kinetic energy of a supernova explosion. The actual available energy will be reduced by a factor of $\sim$10, since most of the neutrinos are radiated in the later phase where the luminosity has declined substantially and the neutrino-heating is no longer efficient. Still, the energy that neutrinos can potentially deposit is much greater than the canonical explosion energy.

The problem with this mechanism is that neutrinos interact only weakly with matter and the neutrino-heating is indeed inefficient. In addition, the cooling of matter occurs simultaneously via the very inverse process of the heating reactions, that is, $p + e \rightarrow \nu_e + n$ and $n + e^+ \rightarrow \overline{\nu}_e + p$. Hence the net heating occurs only between the shock wave and the so-called gain radius, at which the heating is just cancelled by the cooling and the net heating vanishes. The issue is the quantitative assessment of whether the heating is sufficient to revive the shock wave. In fact, this is really a subtle problem. In their numerical experiments, Janka and Müller [23] found the shock revival for otherwise failed explosion models if the neutrino luminosity was enhanced artificially by a few tens percent from the original value. On the other hand, Burrows and Goshy [24] demonstrated by studying static configurations after the shock-stagnation that for a given accretion rate there is a critical luminosity for the shock revival. All we have to attain, then, appears to be this relatively small amount of boost of the neutrino luminosity and energy from the values we have obtained in failed explosion models.

In the last couple of years, both numerics and microphysics have been scrutinized. The former, in particular, has seen major progress [4]–[9]. Since Wilson first proposed the neutrino-heating mechanism [25], neutrino transport has been a formidable task and some type of approximation, the multi-group-flux-limited diffusion approximation as the most familiar example, has been employed even in the one-dimensional (1D) spherically symmetric simulations. This is mainly because neutrinos are not in thermal and/or chemical equilibrium with matter except in the central portion of the core and we have to treat not only the spatial but also the momentum distribution of neutrinos as a function of time. This has changed completely lately. A couple of groups [4]–[7], have published the state-of-the-art direct solutions of the Boltzmann equation for neutrinos, and some of them extended even to 2D computations [8, 9, 26]. Although they have still not found successful explosions, the importance of the accurate treatment of neutrino transfer has been confirmed.

The microphysics such as neutrino reaction rates [27] and equations of state have also been studied in detail. The computation of the electron capture rates for various nuclei as mentioned above is one of them [21]. We have at least two equations of state now available based on different realistic descriptions of nuclear interactions [28, 29]. It is easily understood that the neutrino luminosity and/or energy would be increased if the opacity of hot dense matter were somehow smaller than the standard value that we usually use in the numerical modelling. The correlations originating from nuclear interactions have been expected to be promising in reducing the opacity. Although still uncertain, it has been claimed that the opacity of the nuclear matter in the core could be reduced roughly by half [30]–[33]. Relatively small corrections to the standard approximation such as recoil of nucleons and weak magnetism as well as some new reactions like nuclear bremsstrahlung and pair-annihilation/creations among different neutrino flavours have been incorporated and their importance has been evaluated in the recent 1D computations [34]–[36]. Even after these sophistications, the successful explosion has not been found. It seems that the reduction of the neutrino opacity, if any, should occur in the lower-density region much closer to the neutrino sphere, from which neutrinos flow freely. Otherwise, the

enhancement of luminosity and energy will be nullified as neutrinos diffuse towards the neutrino sphere. If the explosion is to occur in the spherically symmetric collapse, we are still missing some important microphysical elements.

1.2. Multi-dimensional aspects

Ever since SN1987A was observed, most researchers think that the dynamics of a supernova is non-spherical one way or another [37]. Hydrodynamical instabilities are supposed to be mainly responsible for this asphericity. The heating region, for example, tends to have a negative entropy gradient because of the neutrino-heating from beneath. It is also pointed out that the accretion shock is subject to large non-spherical oscillations [38]. The region inside the neutrino sphere is also probably unstable. As mentioned in the previous subsection, the neutrino-heating mechanism is very close to explosion as it is in the spherical collapse. Hence, combined with other phenomena such as hydrodynamical instability, it is expected to have a good chance to give a successful explosion. Many multi-dimensional simulations have been made to address this issue, employing different approximations [23], [39]–[42].

The difficulty of multi-dimensional treatment of neutrino transport hampered the definitive answer to this problem. Although some smooth-particle hydrodynamics (SPH) simulations have found explosions induced by the combination of neutrino-heating and convection in the heating region [39, 43], there has been persistent concern with their approximate treatment of neutrino transfer. Other simulations until recently had similar problems [40]. This situation may change soon. A new generation of multi-dimensional simulations has begun to be published [8, 9, 26]. In these simulations, the dynamics of the whole core is computed with a code implemented with the Boltzmann solver. Although they still employ some approximations, this line of research will soon be pursued by other groups.

According to a recently published result [9], successful explosions are still elusive. It should be mentioned that in their models the convective motions are found both inside the neutrino sphere and in the heating region. Hence the maximal boost of heating is expected from these hydrodynamical motions. What effect the employed approximations have on the results remains to be studied further. However, we may have to look for alternatives to the convection.

Our group has been paying attention to stellar rotation [44]–[46]. Apart from the asphericity owing to the convective motion, it has been also recognized that collapse-driven supernovae are in general globally non-spherical [37]. The best example is again SN1987A, the recent pictures of which clearly show the elongated envelope [47, 48]. The spectropolarimetric observations of other supernovae might also support this claim, though still controversial [49]–[51]. It seems most natural to think that this global asphericity is caused by the rotation of the core. Note, however, that the large-amplitude oscillation of the accretion shock as mentioned above may also lead to the global aspherical expansion of the envelope [38, 52].

If the core rotates rapidly, the centrifugal force flattens the core. Then, neutrinos are emitted preferentially in the direction of the rotation axis. Shimizu *et al* [45] pointed out that this anisotropic neutrino radiation may be advantageous to trigger the revival of a shock wave. This is because neutrino-heating is more efficient near the rotation axis than for the spherically symmetric case and the induced global circulative motion supplies cool matter from the equator and carries away heated matter near the rotation axis, which makes the heating process more efficient as a whole. Kotake *et al* [46] estimated the possible anisotropic pattern and amplitude for various rotation laws by 2D simulations of rotational core-collapse with a simplified treatment

of neutrinos and found that the anisotropy assumed in Shimizu *et al* [45] can be obtained if the core is rotating rapidly with the ratio of rotational energy to gravitational energy, $|T/W| \sim 0.5\%$. This will be detailed in section 3.1.

It should be mentioned that this mechanism is important only when the explosion does not occur without global anisotropy. In fact, Fryer and Heger [43] found a minor effect from the anisotropic neutrino radiation in their SPH simulations, where the explosion occurs as a result of convection-boosted neutrino-heating regardless of rotation. It is also added that the rotation of the core may not be so rapid after all. Recent evolution models by Heger *et al* [53, 55] suggest that the transport of angular momentum during the quasi-static evolutionary phase of the progenitor deprives the core of substantial fraction of its angular momentum, particularly when the magnetic torque is taken into account [54, 55]. If this is really the case, the rotation will play no significant role in the dynamics of core-collapse as shown by Buras *et al* [8] (see also Müller *et al* [56]). We had better bear in mind, however, that the evolution models are based on 1D calculations and have some uncertainties in the mechanism and treatment of angular momentum transport.

In the next section, we will consider the effect of rotation on the accretion shock using the analysis of the static configurations. This is an extension of the study by Burrows and Goshy [24] to the rotational case. We will discuss the change of critical luminosity due to rotation and the possible outcome.

1.3. Magnetic fields

Another possible cause for the non-sphericity of supernovae may be stellar magnetic fields. It is a well known fact that pulsars are magnetized neutron stars. Hence it is expected that the core is also magnetized prior to collapse in general. The issue is the strength of magnetic fields. The canonical value for the pulsar, $\sim 10^{12}$ G, is negligibly small in terms of the effect on the dynamics of collapse. In fact, the magnetic field strength should be $\gtrsim 10^{16}$ G if the magnetic stress is to be comparable with the matter pressure in the supernova core. This is mainly the reason why there have been so few papers published so far on the magnetic supernovae [57]–[62].

It is recognized these days that some neutron stars are indeed strongly magnetized, $\gtrsim 10^{15}$ G. There are about 10 of them. Some of them are soft gamma repeaters and others are anomalous x-ray pulsars or high-field radio pulsars [63, 64]. They are collectively referred to as magnetars. At the moment, they are supposed to be a minor subgroup of neutron stars. The origin of this large magnetic field is so far a mystery. The core might have strong magnetic fields prior to collapse already, although the evolution models by Heger *et al* [55] indicate quite the contrary. The magnetic fields that are weak at first might be somehow amplified during the supernova [65].

Yamada and Sawai [61] considered the former case and studied numerically the effect of magnetic fields on the dynamics of the prompt propagation of a shock wave. Their 2D non-relativistic magnetohydrodynamic (MHD) simulations showed that the combination of rapid rotation, $|T/W| \gtrsim 0.1\%$, and strong poloidal magnetic field, $|E_m/W| \gtrsim 0.1\%$, where $|E_m/W|$ is the ratio of the energy of the magnetic field to the gravitational energy, leads in general to jet-like explosions. They found that the magnetic fields are amplified by the wind-up due to differential rotation as well as by the ensuing MRI-like lateral motions of fluid mainly around the boundary of the inner and outer cores near the rotation axis. Intriguingly, the models with the smallest magnetic fields studied still produced a jet-like explosion although it takes longer to launch the jet. This might suggest that even much smaller magnetic fields could be amplified in the collapsed core and play an important role for explosion. Although we do not know if the

strong magnetic fields are common phenomena for the ordinary supernova, it is interesting to see if strong magnetic fields are helpful for the neutrino-heating mechanism.

Kotake *et al* [62] analysed the models with predominantly toroidal magnetic fields, which will be more realistic as suggested by the evolution models. They paid particular attention to the anisotropy of the neutrino radiation, which will be summarized in section 3.2. We also discuss the effect of strong magnetic fields on the heating rates based on our numerical models and the implication for the pulsar kick velocity.

2. Accretion shock and its revival

In this section, we consider the effect of rotation on the post-bounce quasi-static configurations and the revival of stalled shock. After the shock is stalled, the mass accretion rate and neutrino luminosity change slowly and we can approximately describe the state of the core as a steady accretion flow with a standing shock. Assuming spherical symmetry, Burrows and Goshy [24] sought a series of steady-state solutions and found that for a given mass accretion rate there is a critical neutrino luminosity above which there exists no steady-state solution. Using this fact, they argued that the condition for the revival of the stalled shock is that the neutrino luminosity should exceed this critical value.

In this paper, we extend their analysis to the rotational collapse. We seek steady-state solutions of rotating accretion flows with a standing shock, which is non-spherical in general, by solving 2D time-independent hydrodynamical equations. We investigate the effect of rotation on the accretion flow as well as the critical luminosity of neutrinos based on the solutions. Since our purpose here is not to determine the critical values quantitatively but to see qualitatively how rotation affects the flow and the critical luminosity, we adopt a few assumptions and simplifications in solving the steady flow. Formulations are Newtonian and we do not solve neutrino transport assuming that the neutrino luminosity and energy spectrum do not depend on the radius. Although this is mainly for simplicity, the approximation is justified as our computations are limited to the region outside the neutrino sphere. We take into account only absorptions and emissions of neutrinos on nucleons as for heating and cooling processes. Photo-dissociations are neglected. Although there may exist a region where flows are convectively unstable, it is not taken into account.

The basic equations are given as

$$\frac{1}{r^2}\frac{\partial}{\partial r}(r^2\rho u_r) + \frac{1}{r\sin\theta}\frac{\partial}{\partial\theta}(\sin\theta\rho u_\theta) = 0, \tag{1}$$

$$u_r\frac{\partial u_r}{\partial r} + \frac{u_\theta}{r}\frac{\partial u_r}{\partial\theta} - \frac{u_\theta^2+u_\phi^2}{r} = -\frac{1}{\rho}\frac{\partial p}{\partial r} - \frac{GM}{r^2}, \tag{2}$$

$$u_r\frac{\partial u_\phi}{\partial r} + \frac{u_\theta}{r}\frac{\partial u_\phi}{\partial\theta} + \frac{u_\phi u_r}{r} + \frac{u_\theta u_\phi\cot\theta}{r} = 0, \tag{3}$$

$$u_r\frac{\partial u_\theta}{\partial r} + \frac{u_\theta}{r}\frac{\partial u_\theta}{\partial\theta} + \frac{u_r u_\theta}{r} - \frac{u_\phi^2\cot\theta}{r} = -\frac{1}{\rho r}\frac{\partial p}{\partial\theta}, \tag{4}$$

$$u_r\left(\frac{\partial\epsilon}{\partial r} - \frac{p}{\rho^2}\frac{\partial\rho}{\partial r}\right) + \frac{u_\theta}{r}\left(\frac{\partial\epsilon}{\partial\theta} - \frac{p}{\rho^2}\frac{\partial\rho}{\partial\theta}\right) = \dot{q}, \tag{5}$$

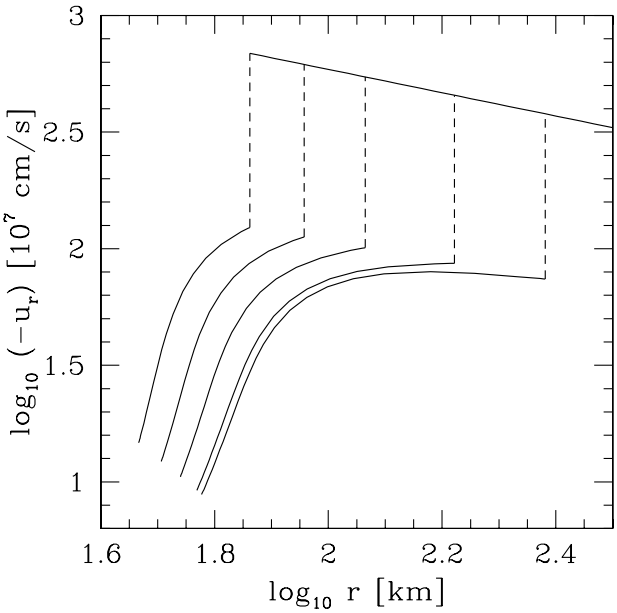

Figure 1. Solution curves of the first branch for steady non-rotating accretion flows with $\dot{M} = 0.2 M_\odot\,\mathrm{s}^{-1}$, $L_{\nu_e} = 5 \times 10^{52}, 6 \times 10^{52}, 7 \times 10^{52}$ and $8 \times 10^{52}\,\mathrm{erg\,s}^{-1}$ and $8.3165 \times 10^{52}\,\mathrm{erg\,s}^{-1}$ (critical value), from left to right. Dashed lines denote shock jumps.

where $\boldsymbol{u}$, ρ, p and ϵ denote velocity, density, pressure and specific internal energy, respectively. The gravitational constant, neutron star mass and net heating rate are represented as G, M, $\dot{q}$, respectively.

The outer and inner boundaries are set at the shock surface and the neutrino sphere, respectively. The neutrino sphere is assumed to be spherical for simplicity, though it is not true in reality. We impose the Rankine–Hugoniot relations as the outer boundary conditions. The upwind flow at the shock wave is assumed to be radial and have a free fall velocity. In the rotating case, the angular velocity just outside the shock wave is obtained based on the assumption of the radial infall and the shell-type rotation at the radius of 1000 km, where the model angular velocity is given. The obliqueness of the shock wave is taken into account. At the neutrino sphere, we impose the inner boundary condition that the density is $10^{11}\,\mathrm{g\,cm}^{-3}$. The more desirable condition would be that the neutrino optical depth from the neutrino sphere to infinity equals 2/3. However, these two conditions are almost identical in the case of spherically symmetric flow and we employ the former condition also in the asymmetric case. As for the temperature of neutrino and the electron fraction, we take the values, $T_\nu = 4.5\,\mathrm{MeV}$ and $Y_\mathrm{e} = 0.5$, in the whole region of calculations.

First, we discuss the case with no rotation, i.e., spherically symmetric flow, which was also investigated by Burrows and Goshy [24]. When the neutrino luminosity is below the critical value, there exist two types of solutions (figures 1 and 2). This is common to the adiabatic accretion flow (the so-called Bondi–Hoyle flow), and is a result of the following feature of the accretion flow. When the flow is subsonic, the accreting gas is first accelerated in the outer region, where the gravitational force is dominant, and later decelerated in the inner region, where the pressure gradient becomes more important. As a result of this flow pattern, we can join the outer supersonic flow with the inner subsonic flow via the shock wave at two points, i.e., in the accelerating regime

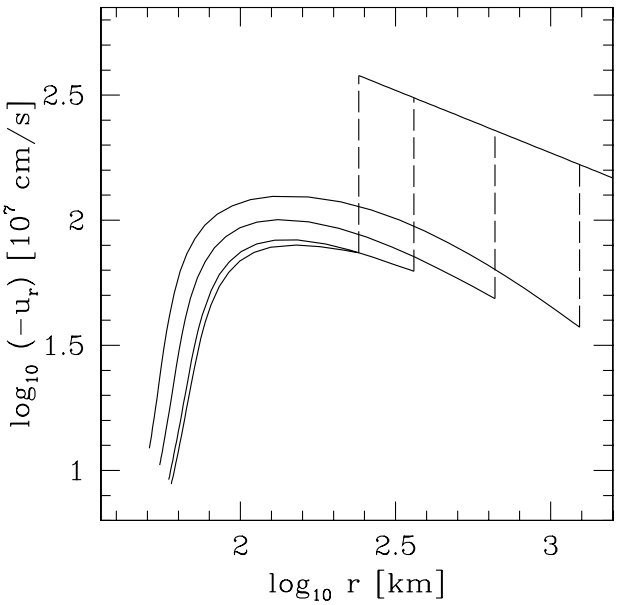

Figure 2. Solution curves of the second branch for steady non-rotating accretion flows with $\dot{M} = 0.2 M_\odot\,\mathrm{s}^{-1}$, $L_{\nu_e} = 6 \times 10^{52}$, 7×10^{52} and $8 \times 10^{52}\,\mathrm{erg\,s}^{-1}$ and $8.3165 \times 10^{52}\,\mathrm{erg\,s}^{-1}$ (critical value), from right to left.

or in the decelerating regime. As the luminosity goes higher, the radius of shock becomes smaller in one of the solutions and gets larger in the other. At the critical luminosity, the radii of shocks in the two solutions merge, and when the luminosity exceeds the critical value, there exists no solution satisfying the boundary conditions, as Burrows and Goshy [24] showed (figure 3). The absence of a solution satisfying the Rankine–Hugoniot relations for the standing shock suggests inevitably that, at this point, the shock is revived and starts to propagate outwards. In fact, when the shock is dislocated either inwards or outwards from the equilibrium position, the downstream pressure becomes always larger than the upstream one. This also suggests the revival of the shock at that point.

Next, we discuss the case of rotation. The centrifugal force plays an important role in the flow in this case. As the theory of Bondi–Hoyle accretion flow tells, it tends to accelerate the subsonic flow and decrease the density and temperature [66]. Since the centrifugal force is greater near the equatorial plane than near the rotation axis, the flows are directed to the equatorial plane (figure 4). At the same time, the shock is deformed into prolate configurations and becomes an oblique shock. As a result, the critical luminosity becomes lower than in the spherically symmetric case (figure 3).

Finally, we discuss what will happen in the rotational case when the neutrino luminosity exceeds the critical value. In the case of spherically symmetric flow, the steady shock condition breaks down on the whole shock surface at the same time. On the other hand, in the case of rotation, the condition is violated pointwisely, first at a certain point on the shock surface in general. Then the shock will start to propagate outwards from that point. In the spherically symmetric flow, we found that, at the critical luminosity, the radii of the shocks in the two branches of solutions coincide with each other. Applying this to the rotational case, we can find at which point on the shock front the steady-state condition breaks down first. We find that this

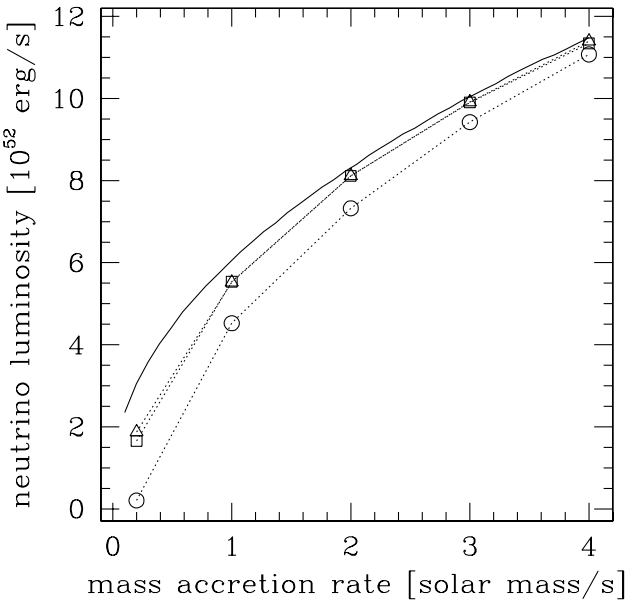

Figure 3. The critical luminosities below which steady accretion flows with a standing shock exist. The solid line corresponds to the spherically symmetric case and open triangles, squares and circles represent the critical luminosities for rotational cases. The rotation frequencies are 0.01, 0.03, 0.10 Hz at 1000 km for triangles, squares and circles, respectively. No steady-state solution exists for a luminosity larger than the critical values.

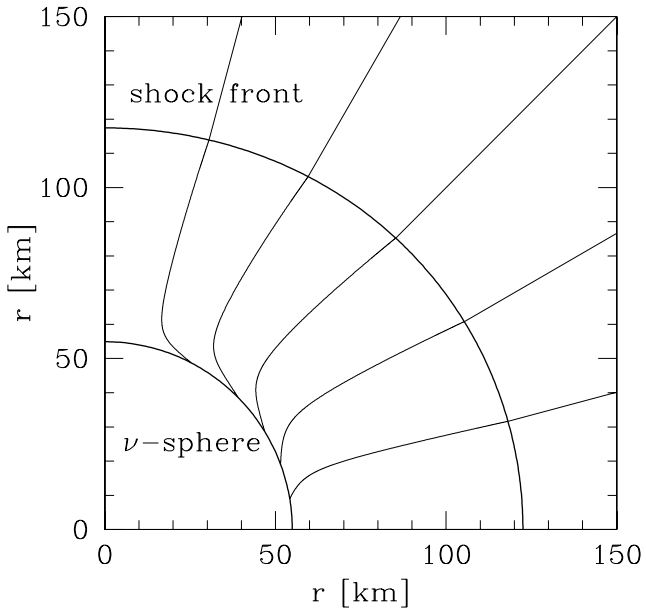

Figure 4. Stream lines for a rotational accretion flow with $\dot{M} = 0.2 M_{\odot}\,\mathrm{s}^{-1}$ and $L_{\nu_e} = 7 \times 10^{52}\,\mathrm{erg\,s}^{-1}$. The rotation frequency is assumed to be 0.1 Hz at a radius of 1000 km.

occurs first at the rotation axis in general. Although time-dependent calculations are necessary to confirm this claim, we think that this suggests that when the luminosity exceeds the critical value in the rotational case, a jet-like explosion will be realized, as suggested by some observations [50]. Detailed results and discussion will be published elsewhere later [67].

3. Rotations and magnetic fields

In this section, we discuss anisotropic neutrino radiations based on our 2D hydrodynamical and MHD simulations.

3.1. Anisotropic neutrino radiation in rotational core-collapse

As stated in the previous sections, recent numerical studies of core collapse supernovae in spherical symmetry have failed to produce explosions [4]–[7]. In the meantime, there are accumulating observations, which require the revision of the spherically symmetric stellar collapse. Spectropolarimetric observations have commonly shown a percent level of linear polarization, which may be interpreted as the asymmetry of core collapse supernovae [49, 51]. It is also well known that SN1987A is globally asymmetric, which is directly observed by the *Hubble Space Telescope* [47, 48]. Provided the facts that the progenitors of collapse-driven supernovae are a rapid rotator on the main sequence [68] and that the recent theoretical studies suggest a fast rotating core prior to the collapse [53] (see, however, [55]), it is important to incorporate rotation in simulations of core collapse.

So far there have been some works devoted to the understanding of the effect of rotation upon the supernova explosion mechanism [8, 43, 44, 57, 59], [69]–[71]. It seems clear that the rotation is not good to prompt shock propagation [44, 71]. This is simply because the centrifugal force tends to halt the core collapse, which then reduces the conversion of gravitational energy into kinetic energy. Here we pay attention to the effect of rotation on the neutrino-heating mechanism. Shimizu *et al* [45] demonstrated that anisotropic neutrino radiations induced by rotation may be able to enhance local heating rates near the rotational axis and trigger globally asymmetric explosions. The required anisotropy of the neutrino luminosity appears to be not very large ($\sim$3%). In their study, the anisotropy of neutrino heating was given by hand and rotation was not taken into account, either. In this paper, we demonstrate how large the anisotropy of neutrino radiation could be, based on the 2D rotational core-collapse simulations from the onset of gravitational collapse of the core through the core bounce to the shock-stall [46]. We not only estimate the anisotropy of neutrino luminosity but also calculate local heating rates based on that.

For the hydrodynamic calculations shown here, we employ the ZEUS-2D code [72]. We made several major changes to the base code to incorporate the microphysics. As for the EOS, we implement a tabulated EOS based on the relativistic mean field (RMF) theory [29] instead of the ideal gas EOS assumed in the original code. We approximate the electron captures and neutrino transport by the so-called leakage scheme. For a more detailed description of the methods, see [46]. As for the initial angular momentum distribution in a core of evolved massive stars, little is known at present about which mode of the instabilities prevails on what time scale during the quasi-static stellar evolution (see [53, 55] for recent developments). Therefore, we assume two possible rotation profiles, shell-type and cylindrical-type. Furthermore, we change the total angular momentum and the degree of differential rotation in a parametric manner. We made the

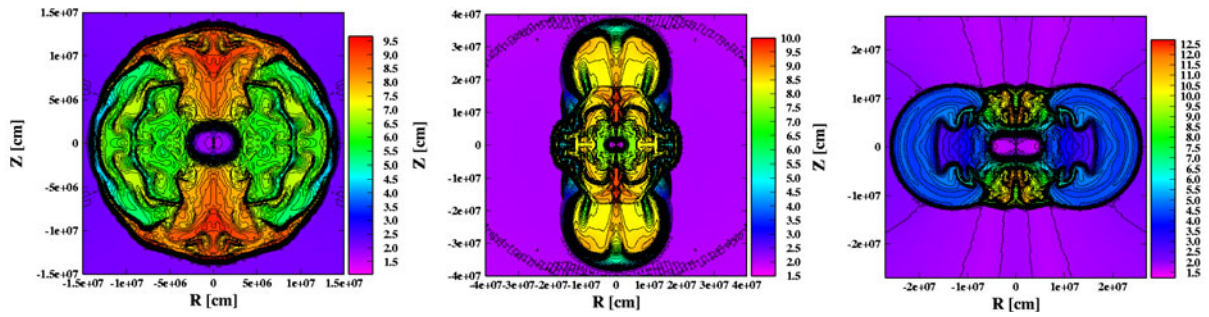

Figure 5. Final profiles of the representative models. They show colour-coded contour plots of entropy (k_B) per nucleon. The initial value of $T/|W|$ is 0.5% for the models of the left (model A) and central panels (model B), 1.5% for the model of the right panel (model C). Here $T/|W|$ is the ratio of rotational to gravitational energy. The model of the central panel has stronger differential rotation than that of the left panel.

pre-collapse models by taking density, internal energy and electron fraction distributions from the spherically symmetric $15M_\odot$ model by Woosley and Weaver [73] and adding angular momentum according to the prescription stated above.

In figure 5, the entropy distributions at the end of computations for some representative models are presented. A variety of the final profiles is immediately seen in the figure. In all the models studied, the shock wave produced by core bounce stalls in the core and no prompt explosion occurs. As the initial rotation rate becomes larger, the shape of the stalled shock wave becomes more oblate due to the stronger centrifugal force (compare the left with the right panel in figure 5). If the initial rotation rate is the same, the shape of the stalled shock is found to be elongated in the direction of the rotational axis as the differential rotation becomes stronger (compare the left with the central panel of figure 5). This is related to the production of high entropy blobs by core bounce. For weak differential rotations, the entropy blob formed near the rotational axis floats up parallel to the axis and then stalls. This makes the shock prolate at first. Then the matter distribution returns to be spherical or oblate due to the centrifugal forces. On the other hand, in the case of strong differential rotations, the shock wave formed first near the rotational axis hardly propagates and stalls very quickly. The high entropy blob begins to grow near the equatorial plane in this case. This then induces the flows towards the rotational axis. As a result, the final configuration becomes prolate. Based on the anisotropic matter distributions after the shock stagnation obtained by these hydrodynamic simulations, we next analyse the neutrino spheres and calculate the degree of anisotropic neutrino radiation.

In the left panel of figure 6, the neutrino spheres for spherical and rotating models are presented. Note that the rotating model in the figure is based on the recent stellar evolution calculation [53]. For the rotating model, it is found that the neutrino sphere forms deeper inside at the pole than for the spherical model. This is a result of the fact that the density is lower on the rotational axis in the rotation models than in the spherical model because the matter tends to move away from the axis due to the centrifugal force. We note that the above features are also true for slower and more rapid rotation models. Furthermore, the configurations are more deformed as the rotation becomes faster due to stronger centrifugal forces. The neutrino temperature profile on the neutrino sphere for the pair is presented in the right panel of figure 6. Note that the neutrino temperature is assumed to be equal to the matter temperature. It is seen from the figure

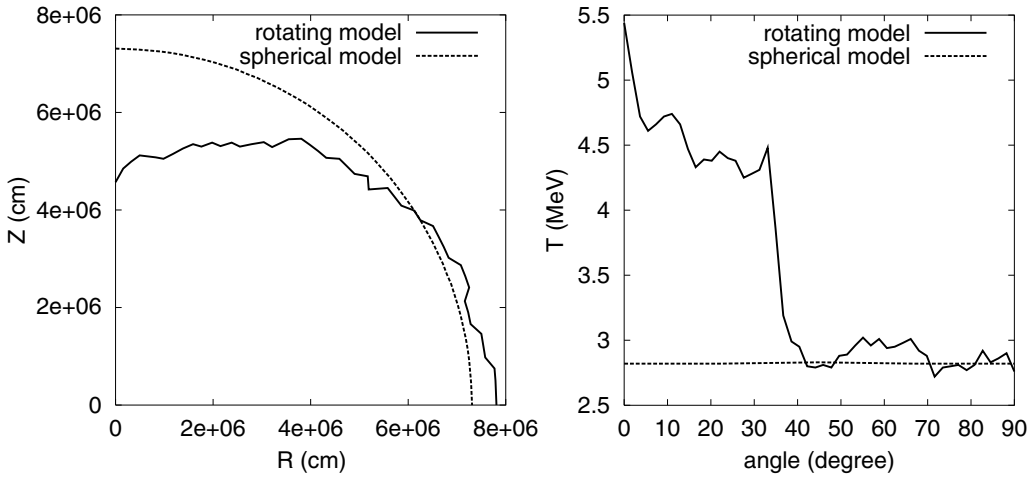

Figure 6. Shapes of neutrino sphere (left panel) and neutrino temperature versus polar angle on the neutrino sphere (right panel) for the rotating model (model A) and the spherical model.

that the temperature varies with the polar angle for the rotating model. The neutrino temperature is higher at the pole for the rotating model than for the spherical model. This can be understood from the fact that the neutrino sphere is formed deeper inside for the rotational model than for the spherical model, as mentioned above.

Based on the above results, we estimate the heating rates outside the neutrino sphere. This is admittedly a very crude estimate, since it is well known [5, 6] that the net heating, the heating minus cooling, becomes positive 50–100 ms after the shock stagnation. We confirmed that the cooling dominates over the heating at the end of simulations in our models also. Since our calculations ended before the heating dominates over the cooling, it is impossible to estimate the location of the gain radius, beyond which the heating dominates over the cooling. Here it is noted that the anisotropy of the heating is found to be similar to that of the cooling in our short runs. It is, thus, expected that the gain radius will be deformed in a similar way in the later phase. If this is true, the bare heating rate discussed below will help us understand the net neutrino heating in the later phase. Bearing this in mind, we consider the bare heating rate for the final configurations (several ten milliseconds after the bounce) in our simulations.

We evaluate the heating rate of the charged-current interaction: $\nu_e + n \rightarrow p + e^-$. The neutrino emission from each point on the neutrino sphere is assumed to be isotropic and take a Fermi–Dirac distribution with a vanishing chemical potential. For the details about the estimation, we refer readers to Kotake *et al* [46]. In figure 7, we show the contour plots of the heating rate for the spherical (top left panel) and some representative rotation models. It is clearly seen from the figure that the neutrino heating occurs anisotropically and is stronger near the rotational axis for the rotation models. This is mainly because the neutrino temperatures at the rotational axis are higher than on the equatorial plane. In addition, the radius of the neutrino sphere tends to be smaller in the vicinity of the rotational axis. As a result, the solid angle of the neutrino sphere is larger when seen from the rotational axis. These two effects make the neutrino heating near the rotational axis more efficient.

By performing the linear analysis for the convective stability in our models, we find that the convective regions appear near the rotational axis (see [46]). This is because the gradient of the

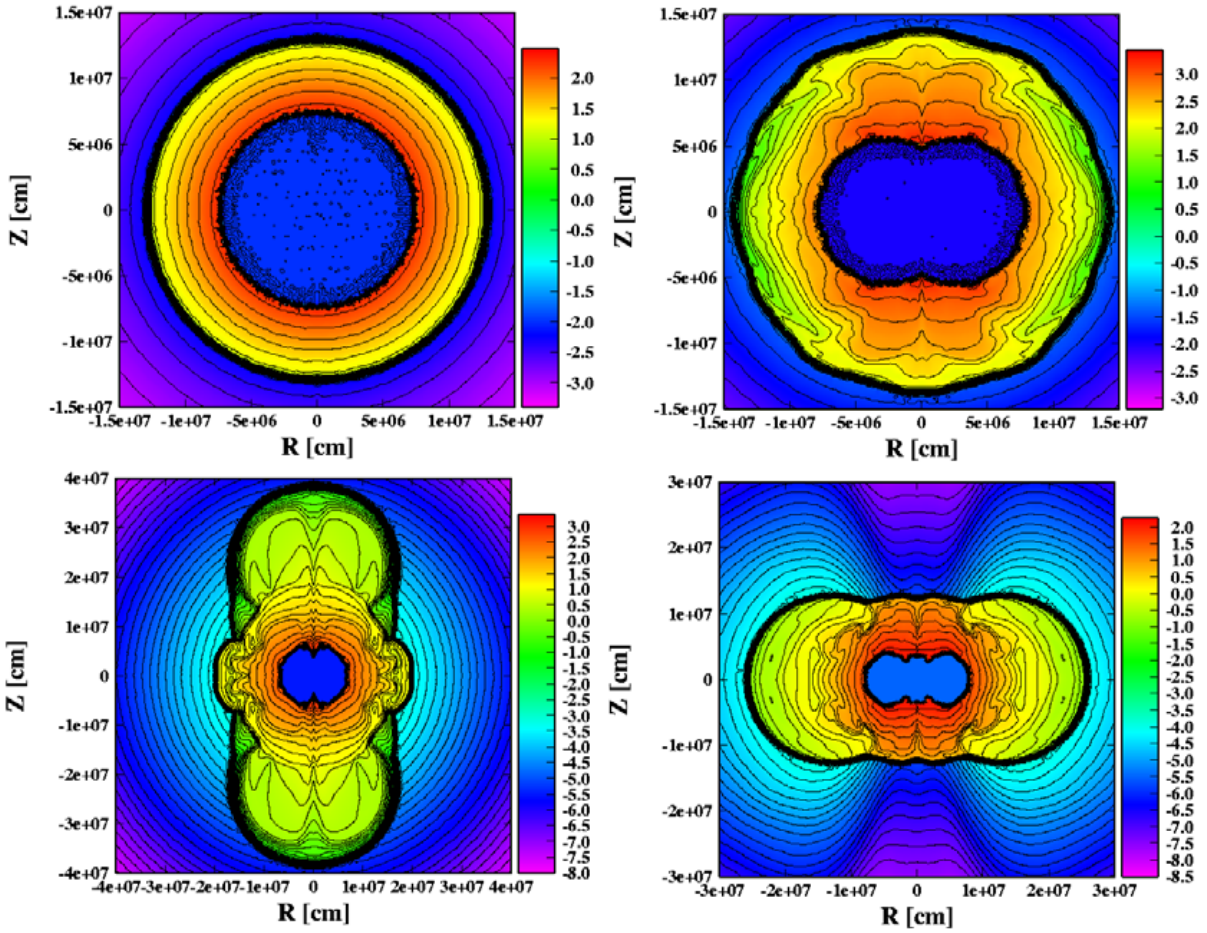

Figure 7. Heating rates outside the neutrino sphere for the spherical model (top left), and also for the models A (top right), B (bottom left) and C (bottom right). All the figures show colour-coded contour plots for the logarithm of the heating rate (MeV nucleon^{-1} s^{-1}). The neutrino sphere and the stalled shock are seen as thick lines separating the bright colour from the dark colour region. Note that the value within the neutrino sphere is artificially modified to dark colours and has no physical meaning.

angular momentum is rather small near the axis and the stabilizing effect of rotation is reduced there. Neutrino heating enhanced near the rotational axis might lead to even stronger convection there later on. Then, the outcome will be a jet-like explosion as considered in Shimizu *et al* [45]. It should be noted that our results suggest that the non-radial neutrino transport should be treated accurately. For this purpose, we are currently preparing 2D radiation-hydrodynamical simulations with an elaborate neutrino transfer scheme [98].

3.2. Effect of magnetic fields

Next we discuss the effect of magnetic fields on the rotational collapse described above. While most of the MHD simulations in the context of core-collapse supernovae choose poloidal magnetic fields as initial conditions [57]–[61], [75, 76], recent stellar evolution calculations

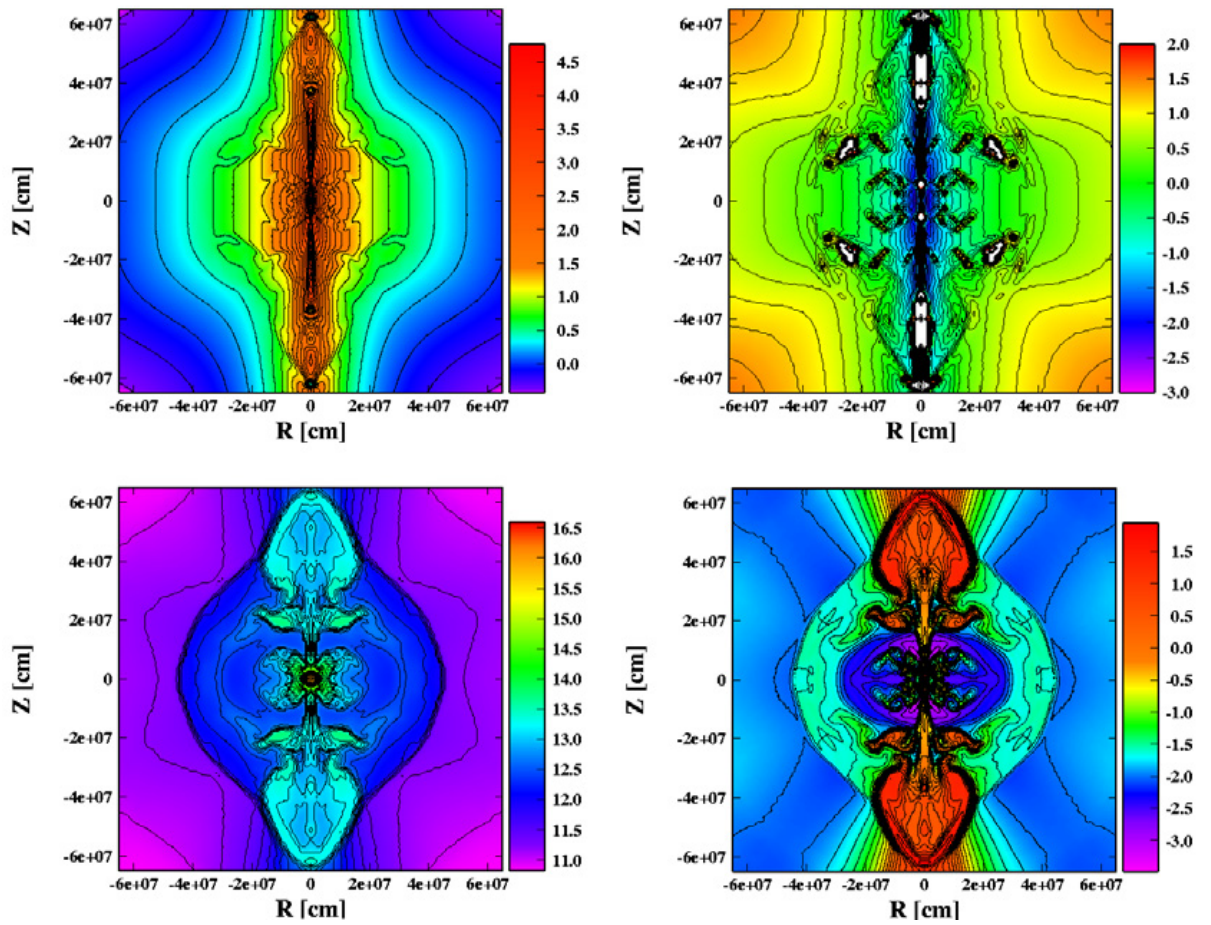

Figure 8. Contour plots of various quantities for the model with the strongest magnetic field in our computations [62]. The top left panel shows the logarithm of the angular velocity (s^{-1}). The top right panel represents the magneto-rotationally unstable regions to non-axisymmetric perturbations. The plot shows the growth time scale (s) of MRI. Note that, in this panel, the regions with white represent stable regions against MRI. The bottom left panel shows the logarithm of magnetic field strength (G). The bottom right panel displays the logarithm of the ratio of magnetic stress to matter pressure in percentage.

show that toroidal magnetic fields may be much stronger than poloidal ones prior to collapse [54, 55]. This situation leads us to investigate the effect of the toroidal magnetic fields on the anisotropic neutrino radiation and convection. We performed a series of 2D MHD core-collapse simulations changing the strength of rotation and the toroidal magnetic fields systematically [62]. We first summarize the results.

The angular velocity profile for the model with the strongest toroidal magnetic fields in our simulations is given in the top left panel of figure 8. The initial values of $T/|W|$ and $E_m/|W|$ are 0.5 and 0.1%, respectively, where $E_m/|W|$ represents the ratio of magnetic field to gravitational field energy. In addition, the initial profiles of rotational and magnetic fields are chosen to be cylindrical with strong differential rotation for this model.

In the top left panel, the negative gradient of angular velocity, $d\Omega/dX < 0$, can be found, where Ω is the angular velocity and X is the distance from the rotational axis. Such a region is known to be unstable to non-axisymmetric perturbations [65, 74]. The characteristic time scale for the growth of the instability called the magneto-rotational instability (MRI) is given as $\tau_{\rm MRI} = 4\pi|d\Omega/d\log X|^{-1}$. The top right panel of figure 8 shows the contour of $\tau_{\rm MRI}$ for the model. The typical time scale is found to be $\sim$O(10) ms near the rotational axis. This suggests that MRI induced by non-axisymmetric perturbations can grow on the prompt shock time scale. The field strengths in the protoneutron star become as high as $\sim 10^{16}$ G (see the bottom left panel of figure 8), and the ratio of magnetic stress to matter pressure gets as high as 0.9 behind the shock wave (see the bottom right panel of figure 8).

As for the anisotropic neutrino radiation, we find that the feature is not changed significantly by the inclusion of very strong toroidal magnetic fields ($\sim 10^{16}$ G in the protoneutron star). Combined with the anisotropic neutrino radiation that heats matter near the rotational axis more efficiently, the growth of the instability is expected to further enhance heating near the axis. Furthermore, the magnetic pressure behind the collimated shock wave is as strong as the matter pressure in the vicinity of the rotational axis. From these results, we expect that the magnetar formation is accompanied by a jet-like explosion if it is formed in the magneto-rotational collapse described above.

In the rest of the section, we present our new results on the effect of poloidal magnetic fields on the neutrino heating. So far we concentrated on the models whose initial magnetic fields are taken to be almost purely toroidal as suggested by the recent stellar evolution calculation [55]. Considering the uncertainties, however, in their models as mentioned before, it should be still important to investigate the effect of poloidal magnetic fields. Here we discuss the model assumed to have strong poloidal magnetic fields ($\sim 10^{12}$ G) prior to core-collapse. In addition, the magnetic field is assumed to be uniform and parallel to the rotational axis initially. During core-collapse, the strength of the magnetic fields substantially exceeds the QED critical value, $B_{\rm QED} = 4.4 \times 10^{13}$ G, and the neutrino reactions are affected by the parity-violating corrections to the weak-interaction rates [77]–[79]. In the following, we estimate the importance of the corrections.

In the left panel of figure 9, the distribution of the poloidal magnetic fields at $t \sim 20$ ms after core bounce is given. The initially uniform magnetic field is deformed to be dipole-like due to core contraction. Using this configuration of magnetic field as a background, we estimate the neutrino heating rate by electron neutrino absorptions on neutron both with and without the parity-violating corrections and compare them by the same procedure as discussed earlier in this paper. As for the cross section with the parity-violating effects, we employ the formula in [78]. The right panel of figure 9 shows the ratio of the heating rate with the corrections to that without the corrections. It is found that the ratio is reduced by $\sim$0.1% due to the corrections near the north pole, whereas it is enhanced $\sim$0.1% in the vicinity of the south pole. If the north/south asymmetry of the neutrino heating persists throughout the later phases, it is expected that the pulsar will be kicked towards the north pole. It is noted that Scheck *et al* [52] recently pointed out that the random velocity perturbation of $\sim$0.1% added artificially several milliseconds after bounce could lead to the global asymmetry of supernova explosion and cause the pulsar-kick. While the orientation of pulsar-kicks is stochastic in their models, the asymmetry of the neutrino heating in the strong magnetic fields considered here will predict the alignment of a pulsar's magnetic axis and the kick velocity. Further numerical investigations are required to see if this is really the case. It is also interesting to study the effect of the anisotropic neutrino

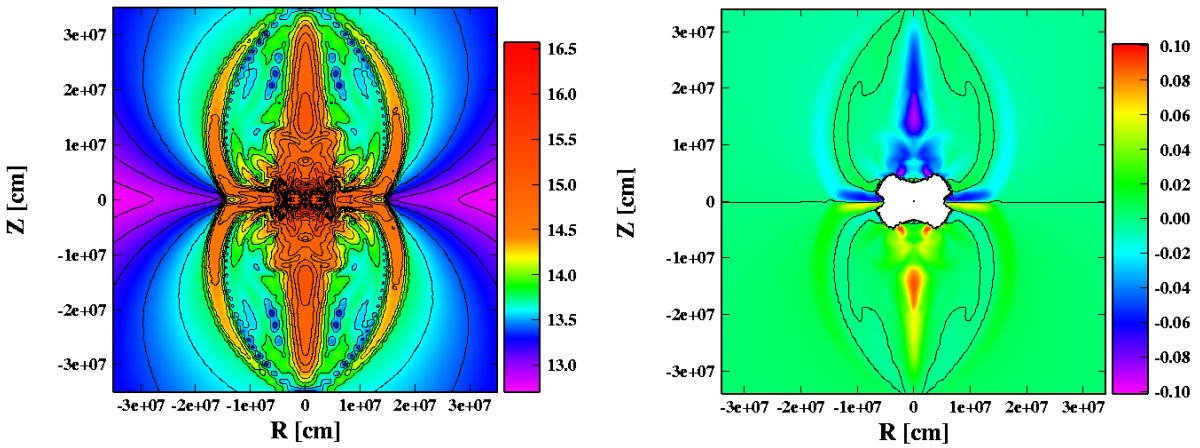

Figure 9. The left panel shows the contour of the logarithm of the magnetic field strength (G). The right panel represents the ratio of the neutrino heating rate with corrections for the parity-violating effect, $Q^{+}_{\nu,\mathrm{B}\neq 0}$, to that without the corrections, $Q^{+}_{\nu,\mathrm{B}=0}$. The values of the colour scale in the right panel are expressed in percentage. Note that the corrections due to the parity-violating effect are $\sim 0.1\%$ on the south and north poles. The surface of the central white region in the right panel represents the neutrino sphere.

radiation in the strong magnetic field on the growth of the convective instability and/or MRI in the later phases [98].

4. Summary

In this article we have reviewed the current status of our theoretical understanding of the collapse-driven supernova. Even the most sophisticated models have not produced a successful explosion so far, although the margin of the theoretical models and the reality seems to have narrowed considerably. We have paid particular attention to the global asymmetry of the dynamics, which may be induced either by rapid rotation or strong magnetic fields of the core. We have solved numerically both static and dynamical equations for rotational cores. Both of them suggest that the rapid rotation and the ensuing anisotropic neutrino radiations are helpful for the shock revival. Strong poloidal magnetic fields may give a substantial kick to the neutron star through the north/south asymmetry of neutrino heating. The origin of the strong magnetic fields remains to be clarified and might be important for the formation of not only magnetars but also ordinary pulsars.

Neutrinos are important from the observational point of view. From the next galactic supernova, we will detect about 10 000 neutrinos, which will reveal the mystery not only of the supernova mechanism but also of neutrino itself. In this respect, the gravitational wave is another important messenger from deep inside massive stars. It will provide us with information, which even the neutrino could not. If the supernova is really asymmetric as considered in this article, we may have a good chance to detect both neutrinos and gravitational waves simultaneously.

We have summarized our recent results on this issue in the appendix, to which we would like to refer interested readers.

As theoreticians, we sincerely hope to be able to make clear the supernova mechanism and the related issues before observations tell us all.

Acknowledgments

This work was partially supported by the Grant-in-Aid for the 21st century COE program 'Holistic Research and Education Center for Physics of Self-organization Systems' and the Grants-in-Aid for Scientific Research (14102004, 14740166, 14079202) of the Ministry of Education, Science, Sports and Culture of Japan. Some of the numerical simulations were done on the supercomputer VPP700E/128 at RIKEN and VPP500/80 at KEK (KEK Supercomputer Projects 02-87 and 03-92).

Appendix. Gravitational waves from the rotational and magnetorotational core-collapse

Here we discuss the gravitational wave from the rotational core-collapse described above. Asymmetric core collapse supernovae have been supposed to be some of the most plausible sources of gravitational radiation for the long-baseline laser interferometers (GEO600, LIGO, TAMA, VIRGO) [80]. The detection of the gravitational signal is important not only for the direct confirmation of general relativity but also for the understanding of supernovae themselves. Combined with neutrino signals, the gravitational wave will enable us to see directly the innermost part of an evolved star, where the angular momentum distribution and the EOS are unknown.

A burst-type gravitational wave is expected to be radiated mainly at the core bounce (see [82, 83] for possible gravitational radiation due to the anisotropic neutrino radiation and the convective motions). Employing the quadrupole formula, we calculated the waveforms of the gravitational wave [84, 85]. First of all, we show the general properties of the waveform with collapse dynamics. The waveform for a typical model is given in the left panel of figure A.1. As the inner core shrinks, the central density increases and the core bounce occurs when the central density reaches its peak at $t_b \cong 243$ ms. At this time, the absolute value of the amplitude becomes maximal. After the core bounce, the core slightly re-expands and oscillates around its equilibrium. As a result, the gravitational wave shows several small bursts and begins to decay. These gross properties are common to all other models. However, there exist some important differences when we compare them in more detail. We will summarize the differences in the following.

In the right panel of figure A.1, the waveform is given for the model, which has a cylindrical rotation law with strong differential rotation. By comparing the left with the right panel of figure A.1, the oscillation period of the inner core for the model in the right panel is clearly longer than that in the left panel. In other words, the pronounced peaks can be seen distinctively in this case. This is because the central density becomes much smaller after the distinct bursts by the strong differential rotation. This effect increases with the initial angular momentum. It is also found that the sign of the second peak is negative in the left panel, while it is

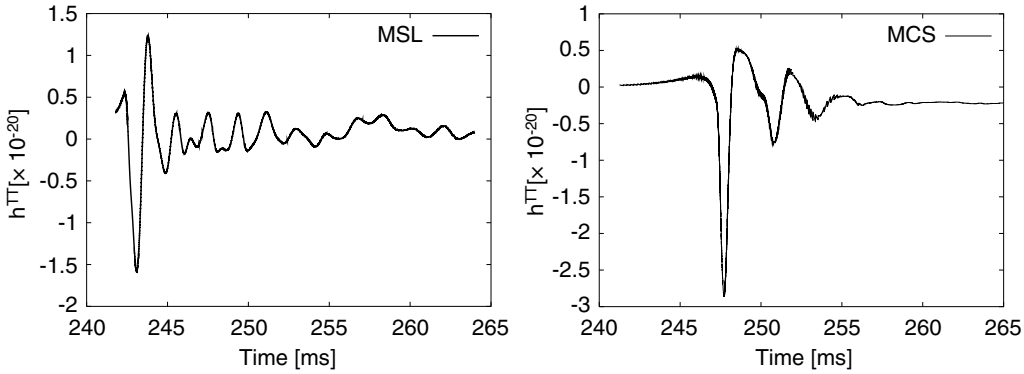

Figure A.1. Time evolutions of the amplitude of gravitational wave for the representative models. Note that the source is assumed to be located at a distance of 10 kpc.

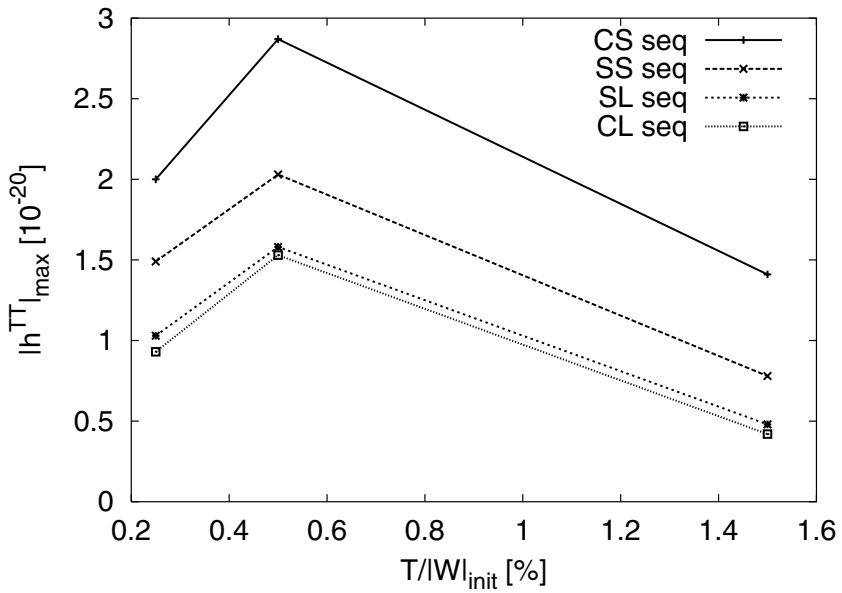

Figure A.2. Relations between $T/|W|_{\rm init}$ and the peak amplitude $|h^{\rm TT}|_{\rm max}$ for all the models [84]. In the figure, CS, SS, SL, CL seq represent the model sequences whose initial rotation profiles differ (see [84] for details). Note that the source is assumed to be located at a distance of 10 kpc.

positive for the model in the right panel. Note that we are speaking of the second peak where the absolute amplitude is the second largest. This characteristic that the sign of the second peak is negative is common to the models with strong differential rotation and the cylindrical rotation law.

Next we discuss the relation between the maximum amplitudes of gravitational wave and the initial $T/|W|$, which is the ratio of the rotational to the gravitational energy. From figure A.2, it is found that the largest amplitude is obtained for the moderate initial rotation rate (i.e. $T/|W|_{\rm init} = 0.5\%$) when one fixes the initial rotation law and the degree of differential

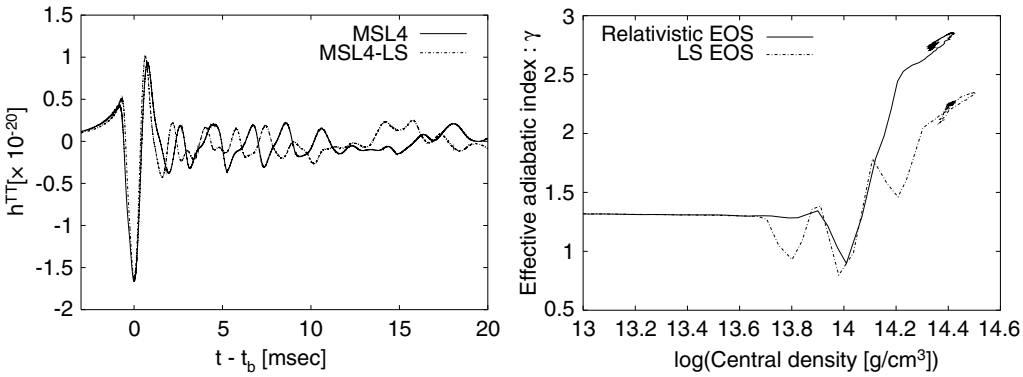

Figure A.3. Waveforms (left panel) for the models with the relativistic EOS (the solid line labelled as MSL4) and with LS EOS (the dashed line labelled as MSL4-LS) and the relation between the central density and the effective adiabatic index γ near core bounce (right panel).

rotation. This is understood as follows. The amplitude of the gravitational wave is roughly proportional to the inverse square of the typical dynamical scale, $t_{\rm dyn}$. Since $t_{\rm dyn}$ is proportional to the inverse square root of the central density ρ, the amplitude is proportional to the density. As a result, the amplitude becomes smaller as the initial rotation rates become larger because the density then decreases. On the other hand, the amplitude is proportional to the quadrupole moment, which becomes larger in turn as the total angular momentum increases. This is because stronger centrifugal forces not only make the mass of the inner core larger, but also deform it. The amplitude of gravitational wave is determined by the competition of these factors. As a result, the amplitudes become maximal for moderate initial rotation rates. According to the study of rotational core collapse by Kotake *et al* [46, 62], considerable anisotropy of neutrino radiation is induced by such rotation rates.

We turn to the effect of the EOS on the gravitational signals. Needless to say, EOS is an important microphysical ingredient for determining the dynamics of core collapse and, eventually, the gravitational wave amplitude. As a realistic EOS, Lattimer–Swesty (LS) EOS [28] has been used in recent papers discussing gravitational radiations from the rotational core collapse [81, 82]. It has been difficult to investigate the effect of EOSs on the gravitational signals because available EOSs based on different nuclear models are limited. Recently, a new complete EOS for supernova simulations has become available [29, 86]. The EOS is based on the RMF theory combined with the Thomas–Fermi approach. By implementing these two realistic EOSs, we look at the differences in the gravitational wave signals. The left panel of figure A.3 shows the waveforms for the models with the relativistic EOS (model MSL4) or the LS EOS (model MSL4-LS). The maximum amplitudes for the two models do not differ significantly. The important difference of the two EOSs is the stiffness. As seen from the right panel of figure A.3, LS EOS is softer than the relativistic EOS. As stated, the amplitude of the gravitational wave is roughly proportional to the central density and, therefore, becomes larger for softer EOS. On the other hand, the amplitude is also proportional to the quadrupole moment, which in turn becomes smaller for softer EOS because the inner core is smaller then. The maximum amplitude is determined by the competition between

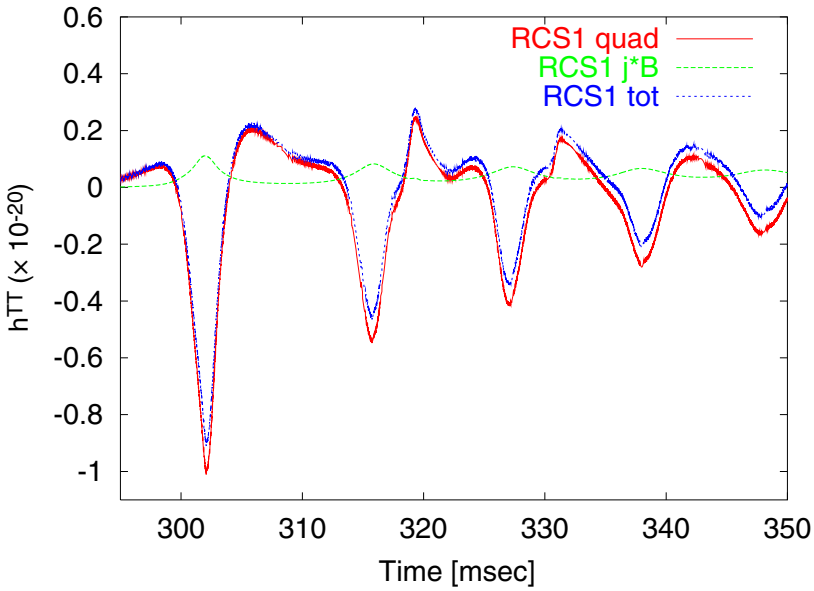

Figure A.4. Waveforms for a model with the strongest magnetic field in our computations [85]. In the figure, quad and $j \times B$ represent the contributions from the mass quadrupole moment and from the electromagnetic field, respectively. The total amplitude is denoted as 'tot'. Note that the source is assumed to be located at a distance of 10 kpc.

these factors. As a result, the peak amplitude becomes almost identical between LS EOS and the relativistic EOS.

We also studied the effect of magnetic fields on the gravitational signals. We derived the quadrupole formula including contributions from the electromagnetic fields [61, 85]. It is found that the amplitude is affected in the strongly magnetized models whose initial $E_{\rm m}/|W|$ is greater than 0.1%. This is natural because the amplitude contributed from the electromagnetic fields should be of the order of $R_{\rm mag} = (B_{\rm c}^2/8\pi c^2)/\rho_{\rm c} \sim 10\%$ $[B_{\rm c}/(\text{several} \times 10^{17}\,\text{G})]^2[\rho_{\rm c}/(10^{13}\,\text{g cm}^{-3})]^{-1}$, with $B_{\rm c}$ and $\rho_{\rm c}$ being the central magnetic field and the central density, respectively. Thus, strongly magnetized models, whose central magnetic fields at core bounce become as high as $\sim 10^{17}$ G, can affect the amplitude. Furthermore, it is found that the contribution of the electromagnetic fields changes in the opposite phase to the matter contribution (see figure A.4). Together with a slight offset of the electromagnetic part, the negative part of the amplitude becomes less negative, whereas the positive part becomes more positive. The peak amplitude at core bounce is lowered by $\sim$10%.

The maximum amplitudes for all our models with or without magnetic fields range from $5 \times 10^{-21} \leqslant h^{\rm TT} \leqslant 3 \times 10^{-20}$ for a source at the distance of 10 kpc. This is almost the same as obtained in previous studies on rotational core-collapse simulations [61], [87]–[93]. The absolute peak amplitudes are presented in figure A.5. If a source is located within 10 kpc, they are mostly within the detection limits of TAMA and the first LIGO now in operation. The result is not changed even if the central core prior to core collapse has very strong magnetic fields of $\sim 10^{14}$ G. As pointed out earlier, we find that the sign of the second peak is negative for the models with strong differential rotation and cylindrical rotation laws, whereas it is positive

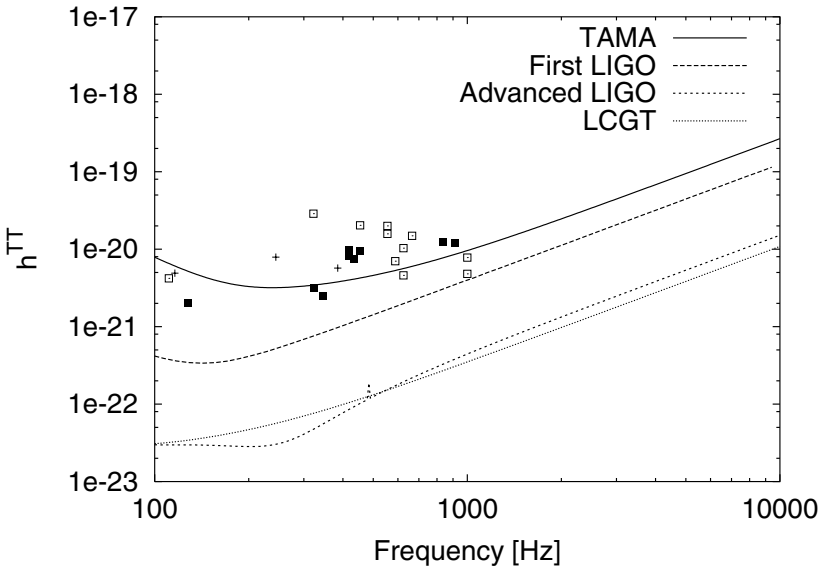

Figure A.5. Detection limits of TAMA [94], first LIGO [95], advanced LIGO [96], and LCGT [97] with the amplitudes from numerical simulations. The open squares represent the maximum amplitudes for all the models, whereas the plus signs and the closed squares stand for the amplitudes of the second peaks for the models with strong differential rotation and cylindrical rotation law and for the other models, respectively. Note that the source is assumed to be located at a distance of 10 kpc.

for the others. The absolute amplitudes of the second peak are also shown in figure A.5. They are also within the detection limit of the first LIGO for a source within 10 kpc. In addition, it seems quite possible for the detectors of next generation such as the advanced LIGO and LCGT to detect the difference in the sign. Therefore, we may be able to obtain in this way the otherwise inaccessible information about the angular momentum distribution of evolved massive stars.

References

[1] Wheeler J C 2003 *Am. J. Phys.* **71** 11
[2] Arnett W D, Bahcall J N, Kirshner R P and Woosley S E 1989 *Ann. Rev. Astron. Astrophys.* **27** 629
[3] Suzuki H 1994 *Physics and Astrophysics of Neutrinos* ed M Fukigita and A Suzuki (Tokyo: Springer) p 763
[4] Rampp M and Janka H T 2000 *Astrophys. J. Lett.* **539** L33
[5] Liebendörfer M, Mezzacappa A, Thilemann F K, Messer O E B, Hix W R and Bruenn S W 2001 *Phys. Rev.* D **63** 103004
[6] Thompson T A, Burrows A and Pinto P A 2003 *Astrophys. J.* **592** 434
[7] Liebendörfer M, Rampp M, Janka H T and Mezzacappa A 2003 *Astrophys. J.* submitted
[8] Buras R, Rampp M, Janka H T and Kifonidis K 2003 *Phys. Rev. Lett.* **90** 241101
[9] Janka H-Th, Buras R, Kifonidis K, Marek A and Rampp M 2004 *Proc. IAU Colloquium 192, 'Supernovae'* ed J M Marcaide and K W Weiler (Berlin: Springer)
[10] Woosley S E, Heger A and Weaver T A 2002 *Rev. Mod. Phys.* **74** 1015
[11] Qian Y-Z 2003 *Prog. Part. Nucl. Phys.* **50** 153

[12] Raffelt G G 2002 *Proc. Texas in Tuscany* December
[13] New K C B 2003 *Living Rev. Rel.* **6** 2
[14] Lazzati D 2004 *Xth Marcel Grossmann Meeting on General Relativity, Rio de Janeiro, Brazil, July 2003*
[15] Hjorth J *et al* 2003 *Nature* **423** 847
[16] Mazzali *et al* 2003 *Astrophys. J. Lett.* **599** L95
[17] Podsiadlowski Ph, Mazzali P A, Nomoto K, Lazzati D and Cappellaro E 2004 *Astrophys. J. Lett.* in press
[18] Fryer C L 1999 *Astrophys. J.* **522** 413
[19] Nomoto K *et al* 2003 *Prog. Theor. Phys. Suppl.* **151** 44
[20] Heger A, Fryer C L, Woosley S E, Langer N and Hartmann D H 2003 *Astrophys. J.* **591** 288
[21] Langanke K *et al* 2004 *Phys. Rev. Lett.* **90** 241102
[22] Bruenn S W 1985 *Astrophys. J. Suppl.* **58** 771
[23] Janka H-Th and Müller E 1996 *Astron. Astrophys.* **306** 167
[24] Burrows A and Goshy J 1993 *Astrophys. J. Lett.* **416** 75
[25] Wilson J R 1982 *Proc. Univ. Illinois Meeting on Numerical Astrophysics*
[26] Livne E, Burrows A, Walder R, Lichtenstadt I and Thompson T A 2003 *Astrophys. J.* submitted
[27] Burrows A, Reddy S and Thompson T A 2004 *Nucl. Phys.* A in press
[28] Lattimer J M and Swesty F D 1991 *Nucl. Phys.* A **535** 331
[29] Shen H, Toki H, Oyamatsu K and Sumiyoshi K 1998 *Nucl. Phys.* A **637** 43
[30] Burrows A and Sawyer R F 1998 *Phys. Rev.* C **58** 554
[31] Reddy S *et al* 1999 *Phys. Rev.* C **59** 2888
[32] Yamada S and Toki H 2000 *Phys. Rev.* C **61** 015803
[33] Mornas L and Perez A 2002 *Eur. Phys. J.* A **13** 383
[34] Thompson T A, Burrows A and Horvath J E 2000 *Phys. Rev.* C **62** 035802
[35] Horowitz C J and Perez-Garcia M A 2003 *Phys. Rev.* C **68** 025803
[36] Keil M Th, Raffelt G G and Janka H-Th 2003 *Astrophys. J.* **590** 971
[37] Wheeler C J 2004 *Proc. on 'Cosmic Explosions in Three Dimensions: Asymmetries in Supernovae and Gamma-Ray Bursts'* ed P Hoeflich, P Kumar and J C Wheeler (Cambridge: Cambridge University Press)
[38] Blondin J M, Mezzacappa A and DeMarino C 2003 *Astrophys. J.* **584** 971
[39] Herant M, Benz W, Hix W R, Fryer C L and Colgate S A 1994 *Astrophys. J.* **435** 339
[40] Burrows A, Hayes J and Fryxell B A 1995 *Astrophys. J.* **450** 830
[41] Keil W, Janka H-Th and Müller E 1996 *Astrophys. J. Lett.* **473** L111
[42] Mezzacappa A *et al* 1998 *Astrophys. J.* **493** 848
[43] Fryer C L and Heger A 2000 *Astrophys. J.* **541** 1033
[44] Yamada S and Sato K 1994 *Astrophys. J.* **434** 268
[45] Shimizu T M, Ebisuzaki T, Sato K and Yamada S 2001 *Astrophys. J.* **552** 756
[46] Kotake K, Yamada S and Sato K 2003 *Astrophys. J.* **595** 304
[47] Pun C S J and The Supernova Intensive Studies (SNIS) Collaboration 2001 *AAS Meeting* 199 94 02
[48] Wang L *et al* 2002 *Astrophys. J.* **579** 671
[49] Wang L, Wheeler J C, Li Z and Clocchiatti A 1996 *Astrophys. J.* **467** 435
[50] Leonard D C, Filippenko A V, Barth A J and Matheson T 2000 *Astrophys. J.* **536** 239
[51] Wang L, Howell D A, Höflich P and Wheeler J C 2001 *Astrophys. J.* **550** 1030
[52] Scheck L, Plewa T, Janka H T, Kifonidis K and Müller E 2004 *Phys. Rev. lett.* **92** 011103
[53] Heger A, Langer N and Woosley S E 2000 *Astrophys. J.* **528** 368
[54] Spruit H C 2002 *Astron. Astrophys.* **381** 923
[55] Heger A, Woosley S E, Langer N and Spruit H C 2003 *Proc. IAU 215 Stellar Rotation* (*Preprint* astro-ph/0301374), to appear
[56] Müller E, Rampp M, Buras R and Janka H-Th 2004 *Astrophys. J.* **603** 221
[57] LeBlanc J M and Wilson J R 1970 *Astrophys. J.* **161** 541
[58] Müller E and Hillebrandt W 1979 *Astron. Astrophys.* **80** 147
[59] Symbalisty E 1984 *Astrophys. J.* **360** 242

[60] Ardeljan N V, Bisnovatyi-Kogan G S and Moiseenko S G 2000 *Astron. Astrophys.* **355** 1181
[61] Yamada S and Sawai H 2004 *Astrophys. J.* in press
[62] Kotake K, Sawai H, Yamada S and Sato K 2004 *Astrophys. J.* in press
[63] Zhang B and Harding A K 2000 *Astrophys. J. Lett.* **535** L51
[64] Guseinov O H, Yazgan E, Ankay A and Tagieva S 2003 *Int. J. Mod. Phys.* D **12** 1
[65] Akiyama S, Wheeler J C, Meier D L and Lichtenstadt I 2003 *Astrophys. J.* **584** 954
[66] Shapiro S L and Teukolsky S A 1983 *Black Holes, White Dwarfs, and Neutron Stars* (New York: Wiley) p 412
[67] Yamasaki T, Yamada S and Kotake K 2004 in preparation
[68] Tassoul J L 1978 *Theory of Rotating Stars* (Princeton, NJ: Princeton University Press)
[69] Müller E and Hillebrandt W 1981 *Astron. Astrophys.* **103** 358
[70] Bodenheimer P and Woosley S E 1983 *Astrophys. J.* **269** 281
[71] Mönchmeyer R M and Müller E 1989 *Timing Neutron Stars, NATO ASI Series* ed H Ögelman and E P J van der Heuvel (New York: ASI)
[72] Stone J M and Norman M L 1992 *Astrophys. J. Suppl.* **80** 753
[73] Woosley S E and Weaver T A 1995 Private communication
[74] Balbus S A and Hawley J F 1992 *Astrophys. J.* **400** 610
[75] Bisnovatyi-Kogan G S and Ruzmaikin A A 1976 *Astrophys. Sp. Sci.* **42** 401
[76] Meier D L, Epstein R I, Arnett W D and Schramm D N 1976 *Astrophys. J.* **204** 869
[77] Horowitz C J and Li G 1998 *Phys. Rev. Lett.* **80** 3694
[78] Arras P and Lai D 1999 *Phys. Rev.* D **60** 43001
[79] Ando S 2003 *Phys. Rev.* D **68** 063002
[80] Cutler C and Thorne K S 2001 *Proc. GR16, Durban, South Africa*
[81] Ott C D, Burrows A, Livne E and Walder R 2004 *Astrophys. J.* in press
[82] Müller E, Rampp M, Buras R, Janka H T and Shoemaker D H 2004 *Astrophys. J.* **603** 221
[83] Burrows A and Hayes J 1996 *Phys. Rev. Lett.* **76** 352
[84] Kotake K, Yamada S and Sato K 2003 *Phys. Rev.* D **68** 044023
[85] Kotake K, Yamada S, Sato K, Sumiyoshi K, Ono H and Suzuki H 2004 *Phys. Rev.* D in press
[86] Sumiyoshi K, Suzuki H, Yamada S and Toki H 2004 *Nucl. Phys.* A **730** 227
[87] Mönchmeyer R, Schäfer G, Müller E and Kates R E 1991 *Astron. Astrophys.* **246** 417
[88] Yamada S and Sato K 1995 *Astrophys. J.* **450** 245
[89] Zweger T and Müller E 1997 *Astron. Astrophys.* **320** 209
[90] Rampp M, Müller E and Ruffert M 1998 *Astron. Astrophys.* **332** 969R
[91] Dimmelmeier H, Font J A and Müller E 2002 *Astron. Astrophys.* **393** 523D
[92] Fryer C L, Holz D E and Hughes S A 2002 *Astrophys. J.* **565** 430
[93] Shibata M 2003 *Phys. Rev.* D **67** 024033
[94] Ando M and TAMA Collaboration 2002 *Class. Quantum Grav.* **19** 1409
[95] Thorne K S 1995 Gravitational waves *Proc. Snowmass 95 Summer Study on Particle and Nuclear Astrophysics and Cosmology* (Singapore: World Scientific) p 398
[96] Weinstein A 2002 *Class. Quantum Grav.* **19** 1575
[97] LCGT Collaboration 1997 *Int. J. Mod. Phys.* D **5** 557
[98] Kotake *et al* 2004 in preparation